EUROPEAN MECHANICAL SCIENCE
e-ISSN: 2587-1110

Research Article

Deposition and study of plasma sprayed Al_2O_3-TiO_2 coatings on AZ31 magnesium alloy

Tuğba Bayram[1], Muhammet Karabaş[2,3,*], Yusuf Kayalı[1]

[1] Afyon Kocatepe University, Metallurgical and Materials Engineering Dept., Afyonkarahisar, Turkiye.
[2] Kırklareli University, Faculty of Aeronautics and Space Sciences, Department of Airframe and Powerplant Maintenance, Kırklareli, Turkiye.
[3](former)Hakkari University, Materials Science and Engineering Dept., Hakkari, Turkiye.

ORCID: T. Bayram (0000-0003-1777-7863), M. Karabaş (0000-0002-0666-6132), Y. Kayalı (0000-0002-2449-7125)

Abstract: In this study, Al_2O_3, TiO_2 and Al_2O_3+ 3wt%TiO_2 coatings were deposited on AZ31 Mg alloy substrate by plasma spraying. The coatings were structurally characterized by scanning electron microscopy and X-ray diffraction. Corrosion experiments were carried out in 3.5% NaCl solution. Adhesion tests were performed according to Daimler Benz VDI-3198 standard. A coating layer of approximately 70 microns in thickness was deposited. High plasma enthalpy caused phase transformations in alumina-based ceramics. As a result of electrochemical corrosion study, it was determined that the coatings increased the corrosion resistance of AZ31 Mg alloy. While the most corrosion resistant coating is Al_2O_3+ 3wt%TiO_2, the weakest coating against corrosion is TiO_2. The adhesion behavior of all coatings to the substrate was at an acceptable quality level.

Keywords: Plasma spraying, Coating, Alumina, Titania, Corrosion

1. INTRODUCTION

Since magnesium (Mg) and its alloys are the lightest engineering materials, they are one of the candidate materials that are likely to be used in many applications. Mg and its alloys are noted for their low density, high specific strength, good machinability, high thermal conductivity, and good vibration and sound damping properties. With these features, it provides many advantages for use in automotive, aviation, home and office tools, chemical and energy industries. However, poor corrosion and wear resistance limits its use. To increase corrosion resistance of Mg, it is easiest to coat it. Many different coatings have been produced on Mg by different methods [1]. Besides cermet coatings such as WC–CrC–Ni and Cr_3C_2–NiCr, Al_2O_3, TiO_2 based coatings were applied with thermal spray to improve the surface properties of Mg and its alloys [2, 3]. Plasma spray stands out in the production of ceramic coatings with its features such as ease of processing and high coating quality. Plasma sprayed ceramic coatings have high adhesion-cohesion strength. In addition, plasma sprayed coatings do not need post-processes such as heat treatment. However, due to the high plasma temperature, it can be difficult to control the phase structure and purity of the sprayed material during the coating process. In addition, materials with low vapor pressure can evaporate in the plasma flame and non-stoichiometric coatings can be formed [4].

Alumina (Al_2O_3) ceramics are widely used in aggressive service conditions with their high temperature resistance, high fracture toughness, good abrasion resistance and good chemical stability. Al_2O_3 is one of the most industrially produced coatings by plasma spraying. Plasma sprayed Al_2O_3 coatings have been the subject of many studies. According to these studies, when Al_2O_3 is sprayed, it can undergo phase transformations due to high plasma enthalpy. Commercial Al_2O_3 powders are produced in the α- Al_2O_3 phase. However, δ and γ Al_2O_3 phases may occur due to phase transformation in coatings according to plasma spraying conditions. The general approach is that these phases do not strongly affect the coating characteristics. However, in some studies, it has been reported that these phases adversely affect the corrosion resistance of the coating in a long time. Titania (TiO_2) is another one of the most widely used ceramics as coating material with its dielectric, mechanical and chemical properties. When TiO_2 is sprayed with plasma, it decomposes depending on the process parameters. Sub-oxide phases may be formed in the coating structure. Therefore, phases with different O/Ti ratios occur. Researchers reported that this ratio is highly effective on the corrosion resistance of the coating [5]. TiO_2 is added between 3wt% and 40wt% to improve the corrosion resistance of Al_2O_3 ceramics against dilute acids. This process creates a phase with Al_2TiO_5 composition in the coating structure. Therefore, the coating structure includes Al-

* Corresponding author.
Email: mkarabas@itu.edu.tr

European Mechanical Science (2023), 7(1): 35-40
https://doi.org/10.26701/ems.1175394
Received: September 15, 2022 — Accepted: February 9, 2023

$_2TiO_5$ phase as well as Al_2O_3 and TiO_2 phases. This complex phase composition significantly affects the coating properties and provides extra corrosion resistance [6].

In this paper, the results of preliminary research are presented. The main aim of the study is to investigate coatability of AZ31 Mg alloy substrate with the Al_2O_3-TiO_2 by plasma spraying. Also, adhesion and corrosion behavior of the coatings was studied. Thus, lighter constructions can be produced by increasing the application field of Mg and its alloys.

2. MATERIALS AND METHODS

In this study, AZ31 Mg alloy sheets with 2mm thickness and 1 cm^2 surface area were used as substrate material. The chemical composition of the AZ31 substrate is given in table 1. The wt% level of alloying elements such as Al (2.5%-3.5%) and Zn (0.6%-1.4%) are in commercial norms [7]. Before the coating production process, the substrate materials were subjected to sandblasting. After that, the substrates were cleaned in an ultrasonic cleaner for 15 minutes in ethanol in order to remove surface contamination.

The cleaned substrates were fixed in the sample holder and get ready for the coating process. Commercial Metco 105 NS Al_2O_3, Metco 102 TiO_2 and Amdry 6200 Al_2O_3+3wt%TiO_2 powders were used as coating feedstock. SEM images and EDS analysis results of the feedstock powders are given in Figure 1. It is seen that the powders are in angular morphology. In addition, unexpected elements were not found in EDS analysis.

Sulzer Metco 9 MBM plasma gun was used in the deposition of the coatings. 730C was chosen as the gun nozzle. The gun speed and motion were adjusted by three-axis CNC robot. Plasma spraying process parameters are given in Table 2.

The microstructure, chemical composition of the feedstock powders and coatings were examined by field emission electron microscopy (SEM, JEOL JSM 7000F), which is equipped with an energy dispersive spectrometer. X-ray diffraction (XRD) with CuKα radiation (Bruker D8 Advance) was used to investigate the crystalline structure of the powders and coatings.

Electrochemical corrosion tests were performed in 3.5% NaCl solution. Measurements in electrochemical corrosion experiments were taken with Gamry reference 600 potentiostat/galvanostat ZRA. Calculations were made with Echem Analyst Soft software. Before starting the corrosion experiments, the samples were ultrasonically cleaned at 35°C with Acetone for 15 minutes, Ethanol for 15 minutes and double-distilled water for 15 minutes. Then it was dried in an oven at 50 °C for 1 hour. The cleaned samples were kept in 3.5% NaCl solution for 1 hour to stabilize. Afterwards, potentiodynamic corrosion experiments were started at room temperature in the same solution. Saturated Calomel Electrode (SCE) was used as the reference electrode. A 1 cm^2 Pt sheet was used as the counter electrode. Corrosion current (Icorr),

Table 2. Plasma spray process parameters.

Parametreler	
Current (A)	500
Primary gas flow rate,Ar (L/dk)	42.5
Secondary gas flow rate, H_2 (L/dk)	7
Carrier gas flow rate, Ar (L/dk)	6.4
Number of passes	12
Spray distance (mm)	75
Gun speed (mm/min)	200
Turntable speed (Hz)	50

Table 1. Chemical composition of AZ31 alloy (wt %).

Spectrum	Al	Zn	Mg	Other(Mn, Si Etc.)	Total
AZ 31	2.48	0.76	94.27	2.49	100.00

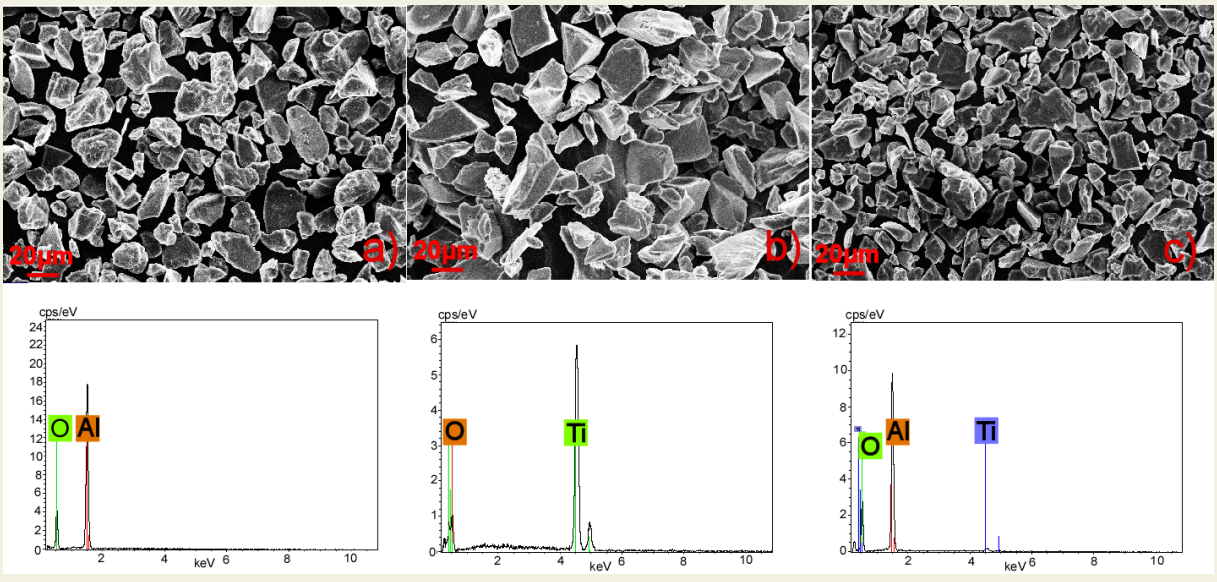

Figure 1. SEM images and EDS analysis graphs of the a) Al_2O_3, b) TiO_2, c) Al_2O_3+%3TiO_2 feedstocks.

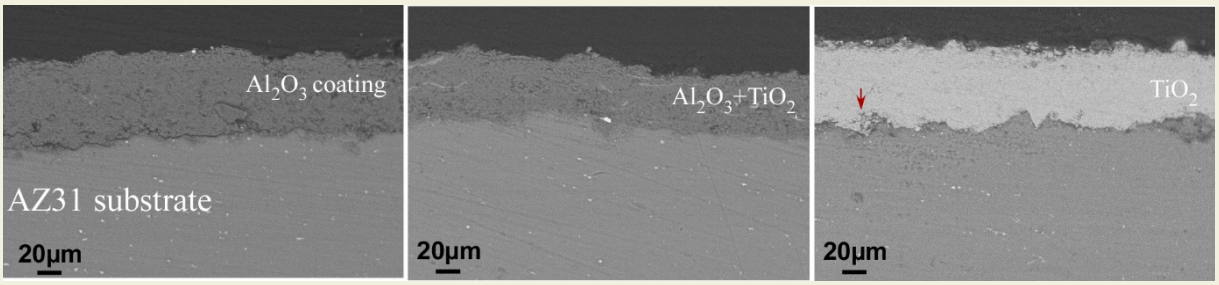

Figure 2. Cross-sectional SEM images of the coatings.

corrosion rate, Polarization resistance (Rp) and corrosion potential (Ecorr) values were recorded from current density-potential curves. Then, the corrosion current density (icorr) was found by dividing the corrosion current by the surface area.

The Daimler-Benz Rockwell-C adhesion test of the coatings was carried out by applying a 980 N load. The indentation zone was examined by SEM and the adhesion of the coatings according to the VDI 3198 standard was evaluated.

3. RESULTS AND DISCUSSION

3.1. Microstructure

The cross-sectional SEM images of the coatings deposited on the AZ31 substrate are given in Figure 2. Considering the adhesion behavior of the coatings to the substrate, it can be said that a crack-free and void-free coating-substrate interface is formed. In this case, a good adhesion regime for coatings can be mentioned. Coating microstructures have the traditional microstructural properties of coatings deposited by plasma spraying. The ceramic layers contain randomly distributed microporosities. A coating layer in the range of 60-70 μm thicknesses was accumulated.

3.2. Phase Structure

The XRD graphs of Al_2O_3 powder and its coating produced by plasma spraying are given in Figure 3. It was determined that the powder has an α-Al_2O_3 mostly phase structure. There is also a little δ-Al_2O_3 phase in powder form. As a result of spraying the powder, a serious phase transformation occurred due to high plasma enthalpy and rapid cooling. In addition, the peak heights decreased and the crystalline phases transformed to the amorphous phase structure. After spraying, δ-Al_2O_3 peak heights increased, α-Al_2O_3 peak heights decreased. The coating phase structure includes amorphous phase, δ-Al_2O_3 and α-Al_2O_3 phases [8, 9].

XRD diffraction patterns of TiO_2 powder and coating are shown in Figure 4. The phase structure of the powder includes two phases, rutile and anatase. When the coating phase structure is compared with initial feedstock powder, it is not possible to talk about a serious difference. No phase transformation occurred after plasma spraying. The coating also contains anatase and rutile phases as in powder [5, 10].

The XRD graphs of the Al_2O_3+3wt%TiO_2 powder and the coating are given in Figure 5. When the powder phase structure is evaluated, there is a phase structure with a majority of α-Al_2O_3. At low altitudes, δ-Al_2O_3 peaks are located. As a result of plasma spraying, a serious phase transformation occurred. It can be said that the α-Al_2O_3 phase turns into amorphous phase as a result of high plasma temperature and rapid cooling of the particles when they reach the substrate. While α-Al_2O_3 peak intensity decreased, δ-Al_2O_3 peak intensity increased because some α-δ Al_2O_3 conversion occurred. In addition, Al_2TiO_5 phase was formed as a result of Al_2O_3-TiO_2 reac-

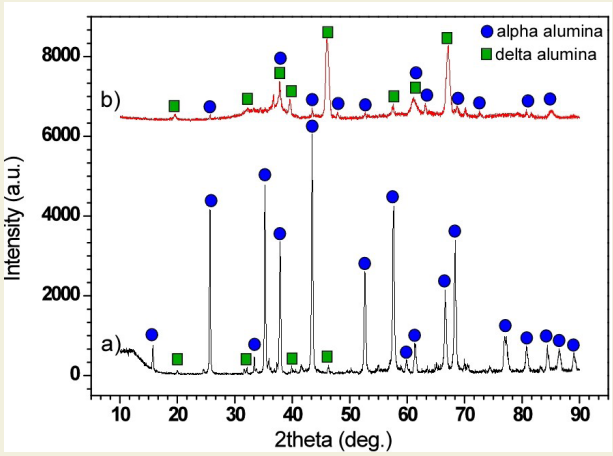

Figure 3. XRD graphs of the Al_2O_3 (a) powder and (b) coating.

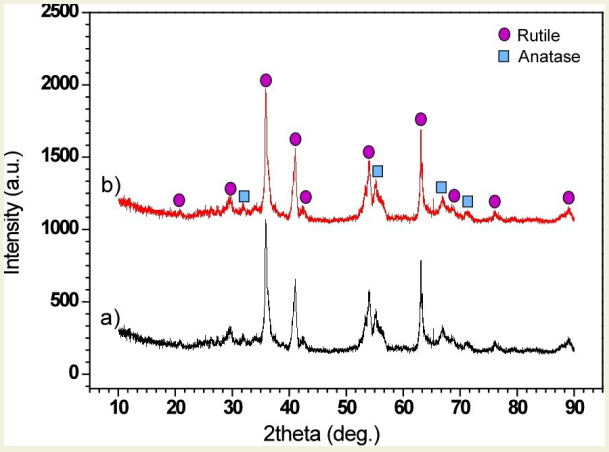

Figure 4. XRD graphs of the TiO_2 (a) powder and (b) coating.

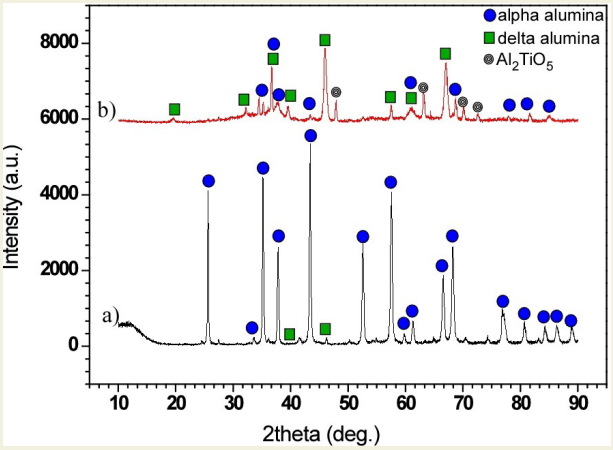

Figure 5. XRD graphs of the Al_2O_3+%3TiO_2 (a) powder and (b) coating.

tion during coating deposition by plasma spraying [8, 11].

3.3. Electrochemical Corrosion Tests

Corrosion variables calculated from the measurements taken during the corrosion tests are given in Table 3. The Icorr corrosion current appears to be highest in the substrate as expected. The corrosion current value decreased with the coating deposition. Among the coatings, the highest corrosion current value was calculated in TiO_2 coating, while the lowest corrosion current value was calculated in Al_2O_3+3wt%TiO_2 coating. On the other hand, the Rp value increased as a result of the coating of the substrate material depending on the Ecorr corrosion potential. While the lowest Rp value was in the substrate material, the highest Rp value was measured in the Al_2O_3+3wt%TiO_2 based coating. When the corrosion rates are evaluated, as expected, a serious decrease occurred as a result of the coating deposition. The corrosion rate of all coatings is lower than the uncoated AZ31 substrate. The highest corrosion rate was found in TiO_2 coating, and the lowest corrosion rate in Al_2O_3+3wt%TiO_2 coating. The Al_2TiO_5 phase in the Al_2O_3+3wt%TiO_2 coating phase structure caused a great decrease in the corrosion rate compared to the Al_2O_3 coating without TiO_2 additives [6]. The standard reduction potentials of aluminum and titanium are -1.66 V and -1.63 V, respectively. These values are very close to each other. This situation showed that the oxidation of Al and Ti in the coating increased in NaCl solution, and reacted with oxygen to form a coating + protective oxide layer on the AZ31 surface. These formations reduced corrosion. Although the Ecor value of the Al_2O_3+TiO_2 coating found from the Tafel curves (Figure 6) was close to AZ31, it was the best coating. The Al_2O_3 coating was more oxidized than TiO_2 and was the coating with the most positive Ecor value. However, the Al_2O_3+TiO_2 coating was slightly oxidized in solution.

Table 3. Corrosion variables of coated and uncoated AZ31 alloys.

%3.5 NaCl	AZ31	TiO_2	Al_2O_3	Al_2O_3+TiO_2
Icorr. (μA)	48.90	30.10	9.130	2.410
Ecorr. (mV)	-1510	-836	-303	-1310
Cor. Rate(mpy)	39.11	18.36	6.691	1.379
Rp(kΩ)	0.0766	12.42	15.97	17.71
Beta A (V/decade)	0.347	0.838	0.804	0.111
Beta C (V/decade)	0.162	2262	0.583	0.254

Figure 5 shows the tafel polarization curves drawn with the measurements taken during the corrosion tests. The gradient regime of the tafel zones and the variation of the polarization zones are consistent with the change in corrosion rates given in Table 3. While the slope of the anodic polarization curves of Al_2O_3 and TiO_2 coatings is higher, the slope of the cathodic polarization curves is higher in AZ31 substrate and Al_2O_3+3wt%TiO_2 coating. In other words, while reduction reactions are dominant in the corrosion of AZ31 substrate and Al_2O_3+3wt%TiO_2, oxidation reactions such as reduction and oxidation are also effective in Al_2O_3 and TiO_2 coatings.

Rp values are also compatible with icorr values. The fact that the Ecor values in all coatings go to more positive potentials shows that there is oxidation on the AZ31 surface with the coating. Anodic (β_a) and cathodic (β_c) Tafel slope values changed according to the properties of the coating material. The highest anodic and cathodic Tafel slopes were detected in the TiO_2 coated sample. However, TiO_2 coating was not as effective in preventing corrosion as Al_2O_3 and Al_2O_3+TiO_2 coating. It is a known fact that aluminum forms a passive film by forming oxide on the surface. The shapes of the Tafel curves are almost the same. This shows that the coatings do not change the corrosion mechanism, they only prevent corrosion by slowing down the anodic and cathodic reactions.

Surface EDX analysis results of the AZ31 and coatings are given in figure 7. It is seen that Na and Cl ions in the corrosion solution are absorbed to the surfaces. The rates of corrosion and the ratios of Na and Cl ions on the surfaces are directly proportional. Na and Cl ions have the lowest proportions and the highest amount of oxygen in the coated magnesium alloy with Al_2O_3+3wt%TiO_2 coating, which has the best corrosion resistance. In the sample coated with Al_2O_3+3wt%TiO_2, the ratios of Na and Cl

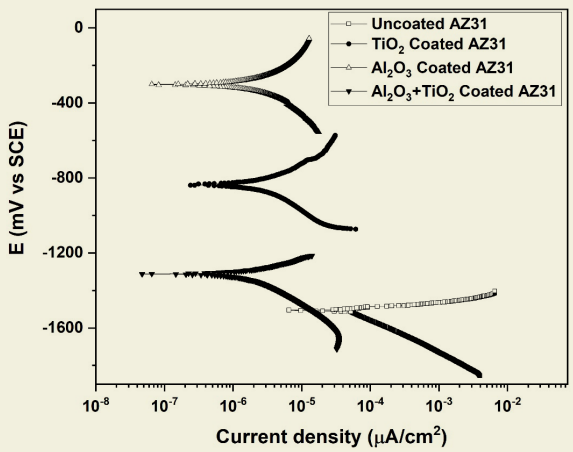

Figure 6. Tafel plots of coated and uncoated AZ31.

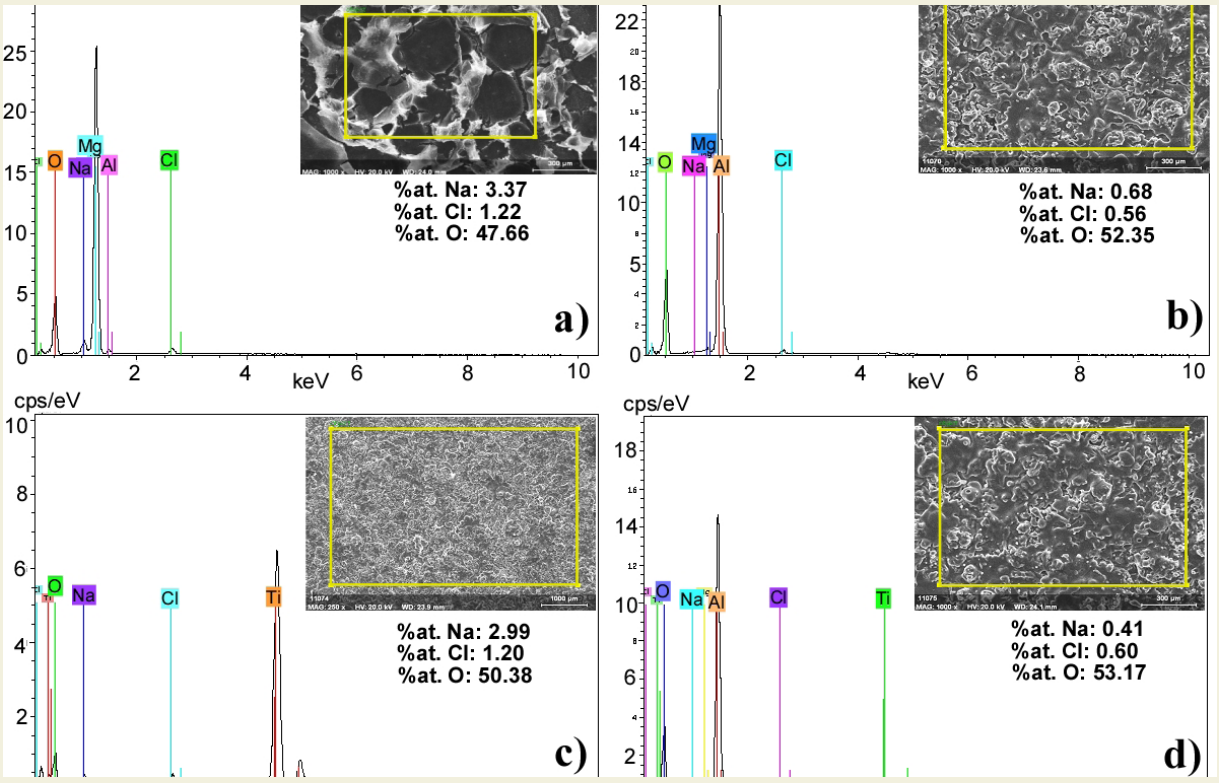

Figure 7. Surface EDX analysis results of the a) uncoated AZ31, b) Al_2O_3 coating, c) TiO_2 coating, d) Al_2O_3+3wt%TiO_2 coating.

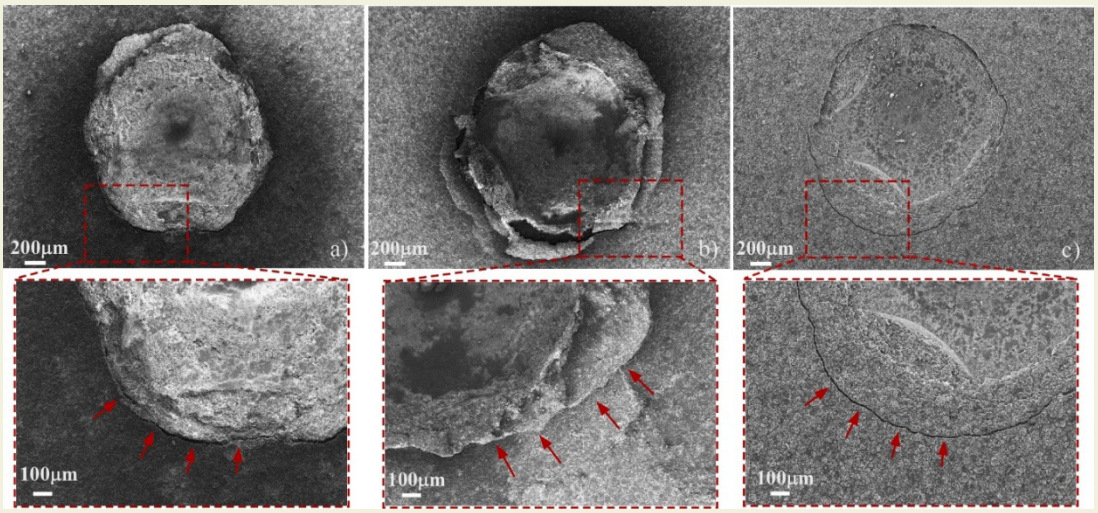

Figure 8. SEM images Rockwell C indentation zone a) Al_2O_3, b) TiO_2, c) Al_2O_3+%wt3TiO_2.

adsorbed to the surface are taken respectively. % Na: 0.41 and Cl: 0.60, the ratios are at least in the untreated magnesium alloy, which has the worst corrosion resistance. % Na:3.37 and Cl: 1.22. While the amount of oxygen on the surface in the uncoated magnesium alloy is 47.46, the amount of oxygen on the surface is 53.17 in the coated magnesium alloy with Al_2O_3+3wt%TiO_2 coating. This contributed to the passivation of the film on the surface by increasing the amount of oxygen on the surface. The film layer that provides this passivation must be sticky, non-porous, chemically inert. If there is a protective film on the coating, the substrate material will not be seriously damaged, corrosion or pitting will not occur, but if the film layer formed contains defects or is discontinuous, the substrate will corrode. To cause pitting, Cl-, SO_4-, Br-, I-, etc. Anions such as ions are adsorbed on the metal surface first. Then, they initiate active dissolution of the metal in the defects present on the metal surface. The presence of second phases where one of the phases has a different chemical composition, microstructure or the formation of micro cells, one of these phases will act as the cathode and the other as the active anode. This will cause preferential dissolution of the one phase acting as the active anode, resulting in preferential, localized dissolution in the material. Al-containing alloys are protected against corrosion by forming a protective layer of Al_2O_3, alumina [12].

3.4. Rockwell C Adhesion Tests

SEM images of the indentation regions are given in Figure 8. All of the coatings exhibited acceptable levels of damage. The damage to Al_2O_3 and TiO_2 is similar. In these coatings, an outward agglomeration occurred in the coatings with the indentation force. There is no separation and crack formation in the coating layer. This situation is directly related to the mechanical properties of the coatings such as fracture toughness and modulus of elasticity. In Al_2O_3+3wt%TiO_2, a circular crack was formed in the area where the indenter sank. Little plastic deformation occurred in the coating with the indentation force [13].

According to all these evaluations, it can be evaluated that all coatings have an acceptable level of adhesion strength. Damages are in HF3-HF4 class according to VDI-3198 standard.

4. CONCLUSION

In this study; AZ31 Mg alloy is coated with Al_2O_3-TiO_2 based ceramics by plasma spraying. Structural characterizations of these coatings were performed and their corrosion behavior was investigated. According to the experimental results, AZ31 Mg alloy can be used for a longer time with plasma sprayed Al_2O_3-TiO_2 coatings in corrosive environments. The lowest corrosion rate was calculated for Al_2O_3+3wt%TiO_2 coating, and the highest corrosion rate was calculated for TiO_2 coating. The adhesion strength of the all coatings is acceptable. However, adhesion strength tests with different methods and a more detailed examination of the coating-substrate interfaces are necessary for further studies. In addition, corrosion tests in more aggressive environments and the behavior of coatings under high temperature conditions can also be investigated. This paves the way for the use of Mg and its alloys in further constructive applications.

ACKNOWLEDGMENTS

This work was supported by Scientific Research Projects Coordination Unit of Hakkari University. Grant number: FM20BAP6.

6. REFERENCES

[1] Gray, J.E., Luan, B., (2002). Protective coatings on magnesium and its alloys — a critical review. Journal of Alloys and Compounds. DOI: 10.1016/S0925-8388(01)01899-0.

[2] Çelik, İ., (2016). Structure and surface properties of Al2O3–TiO2 ceramic coated AZ31 magnesium alloy. Ceramics International. DOI: 10.1016/j.ceramint.2016.05.162.

[3] Jonda, E., Latka, L., Pakiela, W., (2021). Comparison of Different Cermet Coatings Sprayed on Magnesium Alloy by HVOF. DOI: 10.3390/ma14071594.

[4] Heimann, R.B., (2008). Plasma-Spray Coating: Principles and Applications. Wiley.

[5] Gardon, M., Guilemany, J.M., (2014). Milestones in Functional Titanium Dioxide Thermal Spray Coatings: A Review. Journal of Thermal Spray Technology. DOI: https://doi.org/10.1007/s11666-014-0066-5.

[6] Toma, F.L., Stahr, C. L., Berger, M., Saaro, S., Herrmann, M., Deska, D., Michael, G., (2010). Corrosion resistance of APS- and HVOF-sprayed coatings in the Al2O3-TiO2 system. Fraunhofer IWS. DOI: 10.1007/s11666-009-9422-2.

[7] Shankar, S., Nithyaprakash, R., Abbas, G., Naveenkumar, R., Prakash, C., Pramanik, A., Basak, A., (2022). Tribological Behavior of AZ31 Alloy Against Si3N4 Using In-vitro and In-silico Submodeling Approach for Human Hip Prosthesis. DOI: 10.1007/s12633-022-02077-9.

[8] Michalak, M., Latka, L., Sokołowski, P., Candidato, R.T., Ambroziak, S., (2021). Effect of TiO_2 on the microstructure and phase composition of Al_2O_3 and Al_2O_3–TiO_2 APS sprayed coatings. DOI: 10.24425/bpasts.2021.136735.

[9] Mohammadian Bajgiran, M., Rezvani Rad, M., McDonald, A., Moreau, C., (2021). Microstructure, phase and dielectric strength of thermally sprayed alumina layers in coating-based heating systems. DOI: 10.1111/ijac.13731.

[10] Yusuf, Y., Ghazali, M.J., Juoi, J.M., Rahim, T.A., Mustafa, Z., (2022). Plasma-sprayed TiO2 coatings: Hydrophobicity enhanced by ZnO additions. DOI: 10.1111/ijac.14009.

[11] Basha G, M.T., Bolleddu, V., (2021). Characteristics of Thermally Sprayed Alumina-Titania Ceramic Coatings obtained from Conventional and Nanostructured Powders - A Review. Australian Journal of Mechanical Engineering, p. 1-22. DOI: https://doi.org/10.1080/14484846.2021.1876603.

[12] González-Rodriguez, J.G., Colín, J.C., Serna, S., Campillo, B., Albarran, J.L., 2007. Effect of macroalloying with Cu on the corrosion resistance of rapidly solidified NiAl intermetallic in 0.5 M H2SO4. Materials Science and Engineering: A. DOI: 10.1016/j.msea.2006.11.079.

[13] Vidakis, N., Antoniadis, A., Bilalis, N., (2003). The VDI 3198 indentation test evaluation of a reliable qualitative control for layered compounds. Journal of Materials Processing Technology. DOI: 10.1016/S0924-0136(03)00300-5.